Molecular Science

AIMS Molecular Science, 3(3): 439-453.
DOI: 10.3934/molsci.2016.3.439
Received 23 June 2016,
Accepted 16 August 2016,
Published 18 August 2016

http://www.aimspress.com/journal/Molecular

Research article

Cigarette smoke extract is a Nox agonist and regulates ENaC in alveolar type 2 cells

Charles A. Downs[1,2], Abdel A. Alli[3], Nicholle M. Johnson[1,2], and My N. Helms[4,*]

[1] College of Nursing, The University of Arizona, 1305 N. Martin, Tucson, AZ, USA
[2] Division of Translational and Regenerative Medicine, College of Medicine, The University of Arizona, 1501 N. Campbell Ave., Tucson, AZ, USA
[3] Department of Physiology and Functional Genomics, College of Medicine, University of Florida, 135 Center Drive, Gainesville, FL, USA
[4] Department of Internal Medicine, Division of Pulmonary Medicine, School of Medicine, University of Utah, Salt Lake City, UT, USA

* **Correspondence:** Email: my.helms@hsc.utah.edu.

Abstract: There is considerable evidence that cigarette smoking is the primary etiology of chronic obstructive pulmonary disease (COPD), and that oxidative stress occurs in COPD with the family of tissue nicotinamide adenine dinucleotide phosphate (NADPH) oxidase (Nox) enzymes playing a significant role in lung pathogenesis. The purpose of this study was to determine the effects of cigarette smoke extract (CSE) on Nox signaling to epithelial sodium channels (ENaCs). Pre-treatment with diphenyleneiodonium (DPI), a pan-Nox inhibitor, prevented stimulatory effects of CSE on ENaC activity; open probability (Po) changed from 0.36 ± 0.09 to 0.11 ± 0.02; n = 10, p = 0.01 following CSE and DPI exposure. Likewise, Fulvene-5 (which inhibits Nox2 and Nox4 isoforms) decreased the number of ENaC per patch (from 2.75 ± 0.25 to 1 ± 0.5, n = 9, p = 0.002) and open probability (0.18 ± 0.08 to 0.02 ± 0.08, p = 0.04). Cycloheximide chase assays show that CSE exposure prevented α-ENaC subunit degradation, whereas concurrent CSE exposure in the presence of Nox inhibitor, Fulvene 5, resulted in normal proteolytic degradation of α-ENaC protein in primary isolated lung cells. In vivo, co-instillation of CSE and Nox inhibitor promoted alveolar flooding in C57Bl6 mice compared to accelerated rates of fluid clearance observed in CSE alone instilled lungs. Real-time PCR indicates that mRNA levels of Nox2 were unaffected by CSE treatment while Nox4 transcript levels significantly increased 3.5 fold in response to CSE. Data indicate that CSE is an agonist of Nox4 enzymatic activity, and that CSE-mediated Nox4 plays an important role in altering lung ENaC activity.

Keywords: Nox2; Nox4; COPD; lung injury; cell signaling

1. Introduction

Epithelial sodium channels (ENaCs) are composed of three homologous subunits (α, β and γ) and are expressed in tight epithelia lining the luminal surface of the kidney, colon, and lung [1]. ENaC functions to absorb Na^+ at the apical membrane, which is then extruded via the basolaterally located Na^+-K^+ ATPase pump to generate an osmotic gradient that facilitates the movement of water. In the kidney, ENaC plays an important role in maintaining cell volume and total body fluid homeostasis. In the airways and alveoli, ENaC plays a critically important role in regulating the volume of fluid lining lung epithelia. The importance of studying lung ENaC and pulmonary pathogenesis has been shown in α-ENaC knockout mice that die within 40 hours of birth due to an inability to clear lung fluid [2,3]. This animal model highlights the sodium channel's critically important role in edematous lung injury. ENaC has also been shown to play an important role in airway surface dehydration and pulmonary pathogenesis [4-6]; hyper-ENaC activity results in excessively thick mucus in the lungs and increases susceptibility to infection and ultimately inflammation and acute lung injury. Since the rate of movement of Na^+ from the apical membrane to the basolateral compartment translates into net movement of water across the epithelium, it is important to gain a better understanding of molecular regulators of ENaC number (N) and open probability (Po). We have previously shown that a family of Nox enzymes plays an important role in regulating ENaC NPo [7,8], however the effects of Nox enzymatic activity remain unclear.

Nox enzymes are membrane bound complexes that generate reactive oxygen species. There are 7 isoforms (reviewed in [9-11]) and each isoform is believed to be coupled to different agonists thereby promoting varied and specific physiological responses. We, and others, have shown that Rac-1 dependent and constitutively active Nox isoforms (Nox 2 and Nox 4, respectively) have permissive effects on lung and kidney ENaC activity [8,12,13]. In this study, we hypothesize that CSE is an agonist of Nox enzyme activity, and show that the Nox4 isoform amplifies oxidative stress by generating more ROS, which ultimately leads to lung cell dysfunction.

Although smoking and oxidative stress are clear factors in the pathogenesis of COPD [14,15], the patho-mechanisms that ultimately lead to airflow obstruction and lung injury are not clear. Cigarette smoke extract (CSE) has been shown to increase Na^+ transport across airway epithelia [16]. Similarly, Nox-derived ROS plays a permissive role in ENaC regulation [7,8,12,13]. Whether CSE activates tissue Nox enzyme activity has not been specifically addressed. Herein, we characterized the putative roles of Nox2 and Nox4 regulation of ENaC in lung injury and pulmonary disorders that can be attributed to cigarette smoke exposure using single channel analysis and real time measurements of lung fluid clearance.

2. Materials and methods

Animals and primary cell isolation. All procedures were approved by the institutional animal care and use committee and uphold the guidelines set forth by the National Institute of Health. Animals had ad libitum access to water and standard chow.

Eight to ten week old male Sprague Dawley rats were purchased from Charles River (Wilmington,

MA) and used for the isolation of alveolar type 1 (T1) and type 2 (T2) cells. Rat lung tissue slices and primary pneumocytes were prepared using previously published protocols referenced in [12,17], respectively. Twelve-week old female C56Bl/6 mice were purchased from Jackson Laboratory (Bar Harbor, ME) for lung fluid clearance studies, described below.

Reagents. Unless stated otherwise all reagents were purchased from Sigma-Aldrich Chemicals (St. Louis, MO).

Cigarette smoke extract (CSE) preparation. CSE (100%) was prepared as previously described using research grade cigarettes (University of Kentucky, Lexington, KY). The smoke of one cigarette was collected in 10 mL of saline solution (containing: 140 mM NaCl, 5 mM KCl, 1 mM $CaCl_2$ and 10 mM HEPES, with pH = 7.4) using a vacuum syringe and smoking apparatus; the CSE was filter sterilized (0.22 μcron filter). Consistency between batches was obtained by determining the absorbance value (320 nm) as previously reported [16,18].

Electrophysiology. Single channel patch clamp analysis of alveolar T2 cells was performed in the cell attached configuration. Micropipettes were pulled from borosilicate glass capillaries (TW-150, World Precision Instruments), and Gigaohm seals were formed between the cell membrane and the electrode tip. Electrode and bath solutions contained 140 mM NaCl, 5 mM KCl, 1 mM $CaCl_2$ and 10 mM HEPES with pH adjusted to 7.4 with NaOH. Diphenyleneiodonium (DPI) and Fulvene-5 (Nox inhibitor compounds) were applied to cell-attached patch clamp recordings as described in the results section below. Following a control recording period, freshly prepared CSE was applied to the same cell attached recording. Channel activity (NPo), measured as the product of the number (N) of channels and the open probability (Po) was calculated using pClamfit 9.2 data software (Molecular Devices) as previously described in [19,20].

Quantification of ROS. $O_2\cdot^-$ levels were quantified using dihydroethidium (DHE) as described in [7,8,16,19,21].

Radiographic assessment of lung fluid clearance. Assessment of lung fluid clearance was performed as previously described [8]. Briefly, mice received a tracheal instillation of 5 μL/g body weight (100 μL). The saline solution contained 140 mM NaCl, 5 mM KCl, 1 mM $CaCl_2$ and 10 mM HEPES with pH adjusted to 7.4 with NaOH. Immediately following the instillation (Io), animals were x-rayed using an *in vivo* MS FX pro small animal imager (Carestream Health) with an E-Z anesthesia unit (Palmer, PA) attached to deliver 100% oxygen and 2% isoflurane. Radiographs were obtained at 5 min intervals, with 2 min exposure times, for up to 120 min. Settings were as follows: 2X2 binning, 180-mm field of view, and 149-μA x-ray current. X-ray density was quantified using Carestream Health MI software with a defined 5-mm^2 region of interest (ROI). ROI were background corrected then normalized to initial x-ray intensity (Io) in order to make comparisons between time points and treatment groups. I-Io represents the change in lung fluid volume, where I is the x-ray density at a respective time point and Io is the initial x-ray density immediately following the tracheal instillation.

Western blot. T2 cell lysates were electrophoresed on 10% acrylamide gel, transferred to a nitrocellulose membrane (Bio-Rad), and then immuno-blotted. The anti-α-ENaC C-20 (Santa Cruz Biotechnology, Inc) and anti-Nox4 antibodies (Novus Biologicals) are commercially available; IgG-horse radish peroxidase (HRP)-labeled secondary antibody (KPL, Gaithersburg, MD) was used at a concentration of 1 mg/10 mL in buffer and incubated for 1 h at room temperature. HRP signal was detected using CDP-Star chemi-luminescent substrate (Tropix, Bedford, MA). Blots were analyzed on a Carestream imaging station GL 4000 (New Haven, CT) and compatible Carestream Molecular imaging software.

Cycloheximide chase assays. T2 cells were treated in a 0.01% solution of cycloheximide with and without CSE and a Nox-inhibitor (DPI or Fulvene-5). Protein was harvested at 0, 30, 60 and 120 min, followed by immuno-blotting for α-ENaC. Results were normalized to β-actin protein expression levels.

PCR. Total RNA was extracted from T2 cells using an RNeasy isolation kit (Qiagen) following the manufacturer's protocol. RNA was treated with DNaseI and reverse-transcribed using Superscript II RNaseH-reverse transcriptase (Invitrogen). Forward and reverse primers for Nox 2 and Nox 4 were: Nox 2(forward) CAG GAA CCT CAC TTT CCA TAA GAT, Nox 2 (reverse) AAC GTT GAA GAG ATG TGC AAT TGT; Nox4 (forward) CCC AAG TTC CAA GCT CAT TTC C; and, Nox 4 (reverse) TGG TGA CAG GTT TGT TGC TCC T. Threshold levels of mRNA expression ($\Delta\Delta C_t$) were normalized to GAPDH levels, and values represent the mean of triplicate sample ± standard error (S.E.). Data are representative of at least three independent observations.

Statistics. All data are summarized as mean ± S.E. Single comparisons were performed using Student's *t* tests. Multiple comparisons were performed using ANOVA.

3. Results

3.1. Nox inhibition attenuates CSE-induced ENaC activity

Acute exposure to CSE extract elicits an oxidative burden. Whether CSE exposure causes long term oxidative damage by activating tissue Nox enzyme activity, and epithelial cell injury by altering ENaC function, has not been studied. We show the abundance of Nox2 and Nox 4 mRNA from flow-sorted T1 and T2 cells in Figure 1. The transcript data suggest that Nox2 is more abundantly transcribed (and then expressed) in alveolar T2 cells, whereas Nox4 is more robustly expressed in T1 cells. Nox 1 and 3 transcript levels were also measurable in T2 and T1 cells, albeit at significantly lower levels and therefore the data is not shown. Since T2 cells are progenitor cells (which gives rise to T1 cells following injury), and because the biophysical phenotype of T2 cells can be maintained under culture conditions, we continued study of T2 cells using single channel patch clamp analysis.

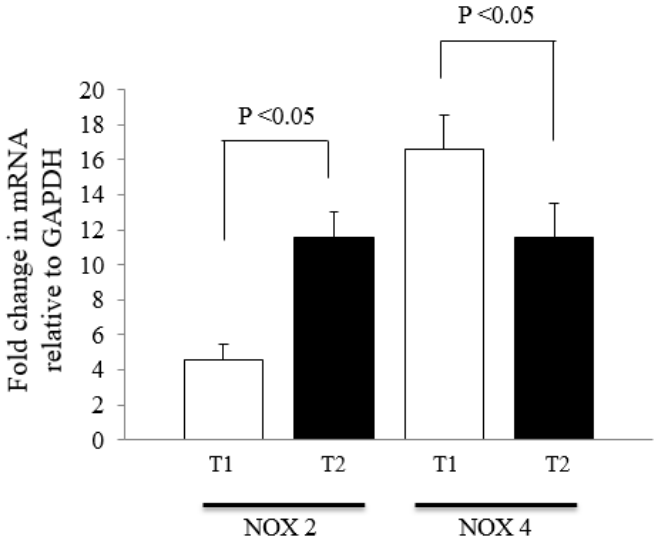

Figure 1. The mRNA expression profile of Nox 2 and Nox 4 obtained from isolated rat alveolar type 1 (T1) and type 2 (T2) cells.

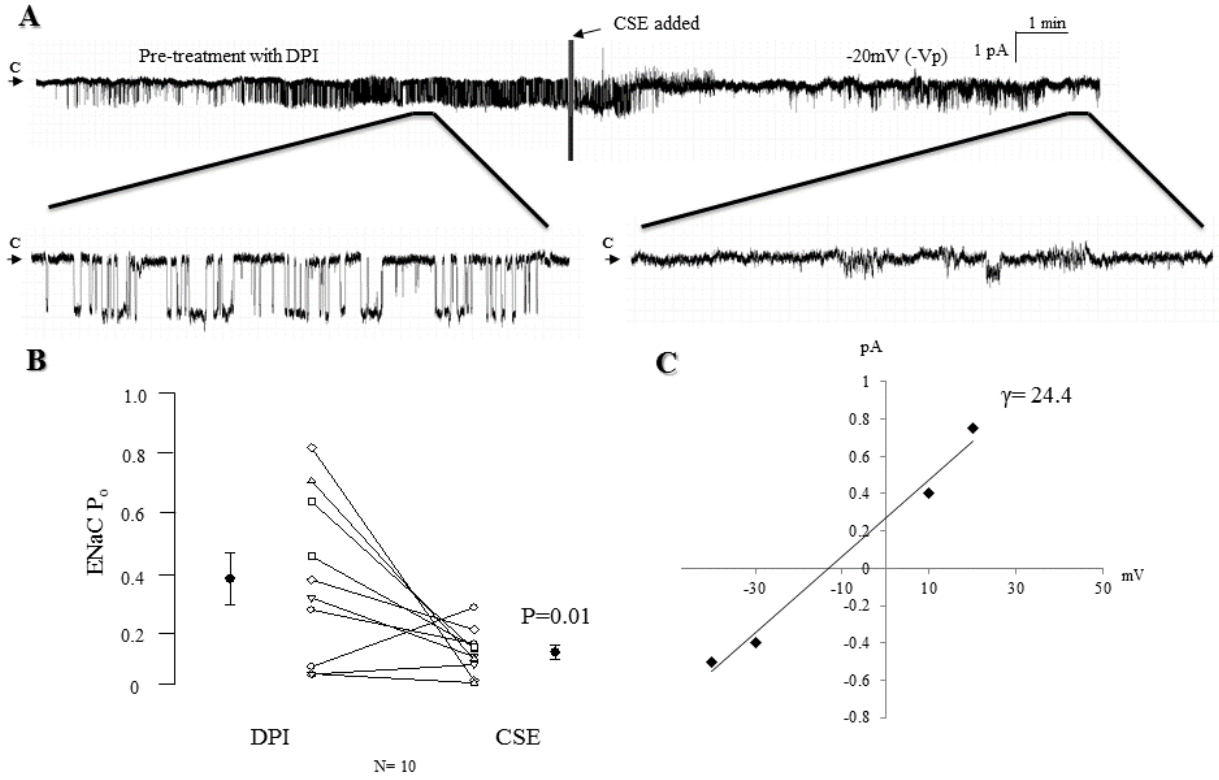

Figure 2. Diphenyliodonium (DPI), a pan-NADPH oxidase inhibitor, attenuates cigarette smoke extract (CSE)-induced ENaC activity in isolated rat alveolar type 2 (T2) cells. (A) Representative single channel recording of a primary alveolar T2 cell pre-treated with 50 μM DPI then challenged with CSE. Arrow represents the closed (c) state with downward deflections indicating channel opening (−20 mV (−Vp)). (B) Line graph showing that CSE challenge decreases ENaC open probability (P*o*) from 0.36 ± 0.09 to 0.11 ± 0.02 when pre-treated with DPI. $n = 10$, $*p < 0.05$. (C) IV curve demonstrating a non-selective cation channel with a unitary conductance (γ) = 24.4 pS.

We evaluated the effect of pretreating T2 cells with 50 μM pan Nox inhibitor compound, DPI, prior to CSE exposure. In Figure 2A we provide a representative single channel recording taken from an isolated T2 cell pre-treated with DPI (50 μM) and then exposed to freshly prepared CSE (where indicated on the trace). Plotting the voltage and current relationship (Figure 2B) shows a non-selective cation channel with a unitary conductance of 24.4 pS evaluated in the representative recording shown. CSE exposure alone significantly increases ENaC Po [4]. In the setting of DPI however, ENaC Po decreased from 0.36 ± 0.09 to 0.11 ± 0.02 following CSE exposure (Figure 2B, $p = 0.01$). Together, the data sets indicate that major Nox isoforms expressed in the alveolar epithelium are needed to activate ENaC activity following oxidative exposure in the lung, since pan-Nox inhibition attenuates CSE-induced activation of ENaC.

Next, we used a recently developed Fulvene compound that inhibits both Nox2 and Nox4 activity with greater specificity compared to DPI compound [3]. Figure 3 is a time-course evaluation of CSE induced activation of ENaC, which persisted for up to 1 h of recorded observation (top trace). This is compared to a significantly sustained inhibition of channel activity when cells were treated with CSE

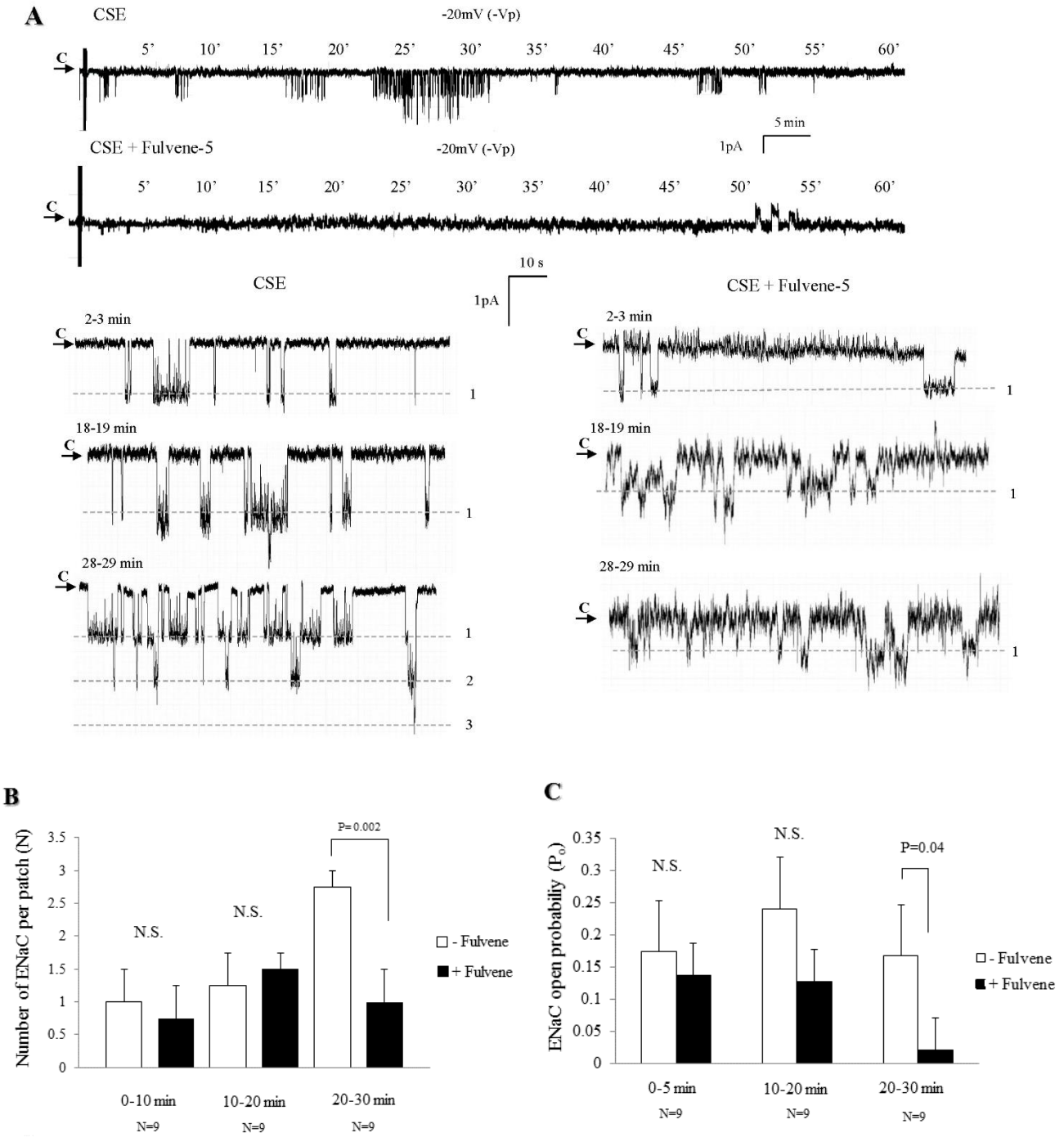

Figure 3. Fulvene-5 attenuates CSE-induced effects on ENaC activity. (A) Representative single channel recordings of a primary alveolar T2 cells treated with CSE with and without Fulvene-5. Arrow represents the closed (c) state with downward deflections indicating channel opening (−20 mV (−Vp)). Enlarged portions of the representative recordings taken between 2–3, 18–19 and 28–29 min. (B) Results of 9 independent observations shown on a bar graph with *y*-axis = Number of ENaC per patch (N); open bars are without Fulvene-5, filled bars are with Fulvene-5. Fulvene-5 treatment reduced ENaC number at 20–30 min; $p = 0.002$. (C) Results of 9 independent observations shown on a bar graph with *y*-axis = ENaC open probability (P*o*). Fulvene-5 treatment significantly decreased ENaC P*o* from 0.18 ± 0.08 to 0.02 ± 0.08 ($p = 0.04$) at 20–30 min of CSE exposure.

in the presence of 10 μM Fulvene 5 (bottom trace). Figure 3A also shows enlarged portions of the CSE and CSE + Fulvene recordings, respectively, to show details of channel closed state and inward current. In Figure 3B and C we report average ENaC N and Po, respectively, obtained in independent single cell recordings.

The data presented in Figure 3 suggest that CSE serves as an agonist for Nox-derived ROS production in lung epithelia and are in line with previous reports showing ROS upregulation of ENaC activity. In order to further implicate CSE's agonistic effects on Nox activity, we exposed primary rat alveolar T2 cells to 1% CSE, 1% CSE with 10 μM Fulvene-5 or 1% CSE with 50 μM DPI and then measured ROS levels (Figure 4). CSE exposure significantly increased cellular ROS production (p = 0.004), whereas concurrent treatment with a Nox inhibitor attenuated ROS production. The data supports a novel signaling pathway in which CSE increases Nox2- and Nox4-derived ROS.

Next, in order to better understand the mechanism of CSE-induced Nox2 and Nox4 isoform regulation of lung ENaC activity, we conducted cycloheximide (CHX) chase assays.

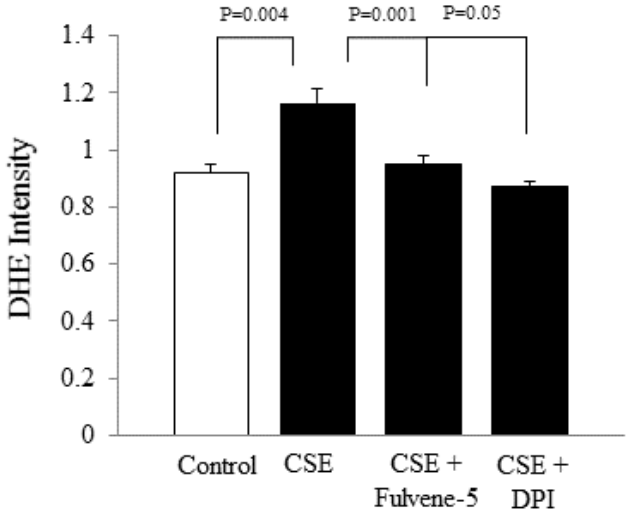

Figure 4. CSE exposure induces ROS production by NADPH oxidases. Measurement of superoxide ($O_2^{\cdot -}$) production in primary T2 cells under control, CSE, CSE with Fulvene-5 and CSE with DPI treatment conditions. CSE significantly increased ROS production (p = 0.004) while concurrent treatment with Fulvene-5 (p = 0.001) or DPI (p = 0.05) significantly decreased CSE-induced ROS production.

3.2. CSE-induced, Nox-generated ROS regulate ENaC protein degradation

In Figure 5A, primary rat alveolar type 2 cells were treated with CHX (a protein synthesis inhibitor) in the setting of CSE or CSE with either Fulvene-5 or DPI and evaluated the rate of proteolytic degradation of the cleaved form of α-ENaC (~65 kDa). The half-life of α-ENaC has been reported to be between 40–120 min [5,14,17] and has been recapitulated in Figure 5A–B under the CHX panels. CSE treatment in the CHX studies inhibited the proteolytic degradation of α-ENaC. However, CHX chase assays in which CSE treatments were combined with Nox inhibiters (DPI and Fulvene-5) showed accelerated rates of α-ENaC degradation that were similar to control half-life values. In Figure 5C we show that Fulvene-5 and DPI treatments increased the amount of total ubiquitinated protein compared to CSE (only) treated cells.

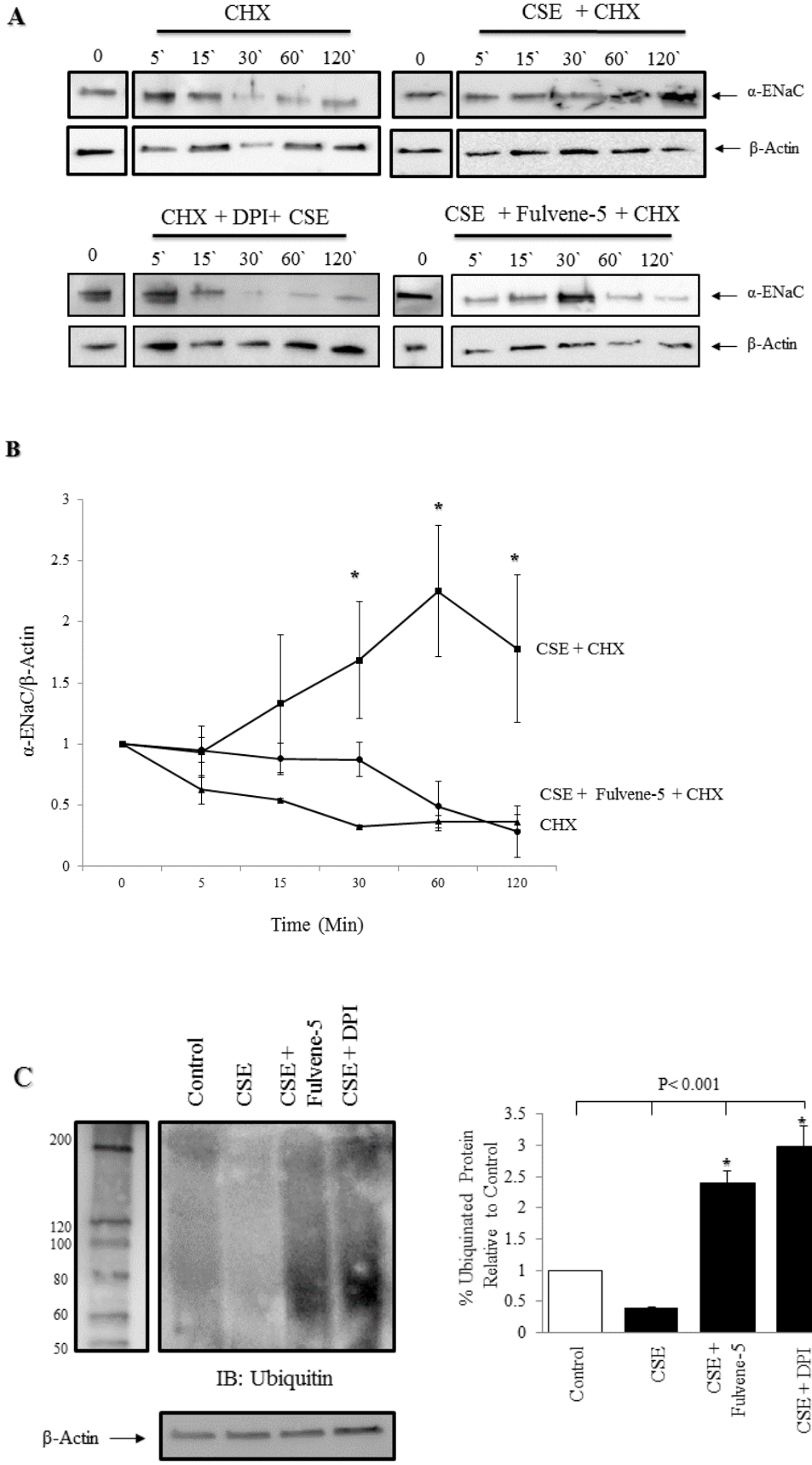

Figure 5. Nox inhibition attenuates effects of CSE on ENaC degradation. (A) Cycloheximide

(CHX) chase performed in the presence of 1% CSE, 1% CSE with 10 μM Fulvene-5 or 1% CSE with 50 μM DPI. Representative immunoblots of α-ENaC and β-actin loading controls provided. (B) Averaged results from 4 independent observations normalized for β-actin shown of *y*-axis, and *x*-axis represents ENaC half-life (min). * indicates $p < 0.05$. (C) Representative immunoblot of ubiquitin from T2 cells treated with 1% CSE, 1% CSE with 10 μM Fulvene-5, or 1% CSE with 50 μM DPI. Averaged results of 4 independent observations normalized to β-actin shown on *y*-axis. Treatment with CSE alone significantly decreased protein ubiquitination; Nox inhibition attenuated CSE-induced inhibition of ubiquitination. * indicates $p < 0.05$ compared to CSE alone.

3.3. CSE affects Nox 2 and Nox 4 transcript levels

In Figure 6, we evaluated the effects of an acute exposure to CSE on Nox2 and Nox 4 transcript. Nox 2 mRNA levels were not affected by CSE exposure (Figure 6A). However, Nox 4 mRNA significantly increased with CSE exposure, an effect that was abrogated with concurrent treatment with Fulvene-5 (Figure 6B). Based on the changes observed in tissue Nox expression following CSE exposure, we conclude that Nox4 is the primary isoform responsible for changes in net salt and water absorption across lung epithelia following CSE exposure. Neither DPI nor Fulvene-5 alone affect Nox2 or Nox4 expression.

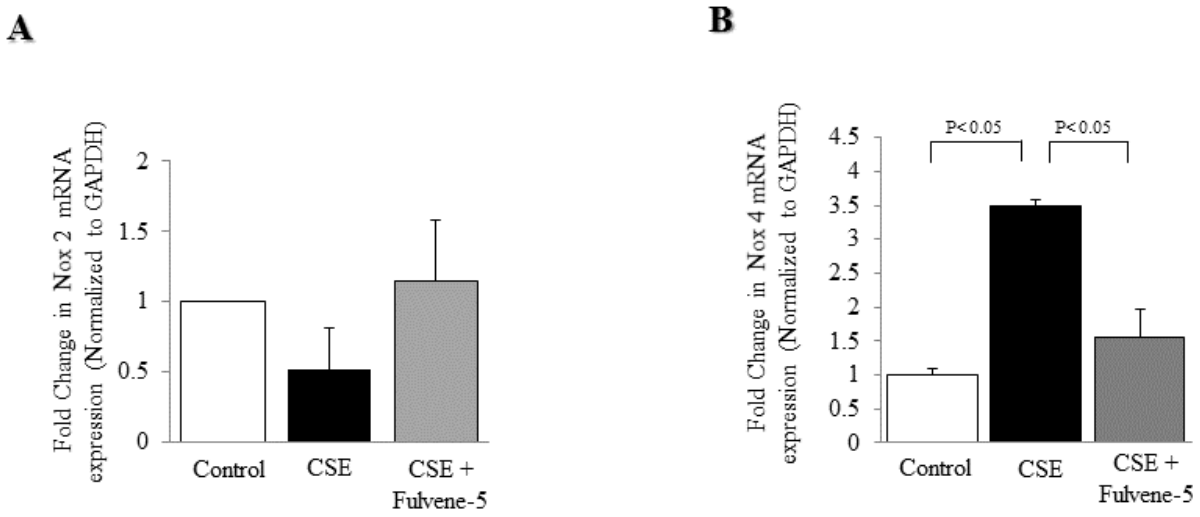

Figure 6. The Effect of CSE on Nox 2 and Nox 4 expression. (A) Nox 2 mRNA levels obtained from rat primary alveolar T2 cells following treatment with 1% CSE or 1% CSE with 10 μM Fulvene-5. (B) Nox 4 mRNA levels obtained from rat primary alveolar T2 cells following treatment with 1% CSE or 1% CSE with 10 μM Fulvene-5. CSE treatment increased Nox 4 mRNA ($p < 0.05$).

3.4. CSE-induced, Nox-generated ROS play a significant role in oxidative regulation of ENaC and lung fluid clearance

Using a novel radiographic technique, we assessed for changes in lung fluid volume over time in mice receiving a tracheal instillation of saline (open circle), CSE (filled square) or CSE with either

DPI (filled circle) or Fulvene-5 (filled diamonds) (Figure 7). CSE significantly increased lung fluid clearance compared to saline controls beginning at approximately 115 min into the experiment. The addition of DPI significantly inhibited fluid clearance by 75 min, an effect that continued throughout the 4 h observation. Fulvene-5 treatment resulted in a significant reduction in lung fluid clearance within 15 min followed by a dramatic reduction in fluid clearance occurring at 65 min; the effect persisted throughout the 4 h observation.

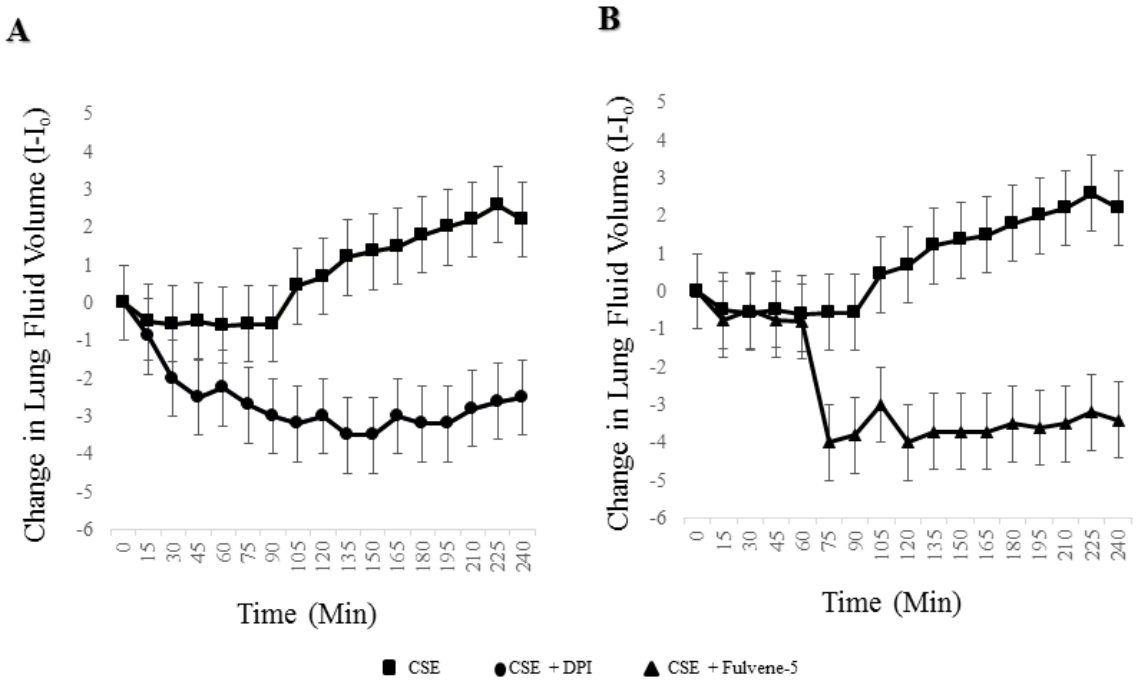

Figure 7. Nox-inhibition attenuates CSE-induced lung fluid clearance *in vivo*. Line graphs depicting changes in lung fluid clearance in mice receiving a tracheal challenge of (A) CSE versus CSE with 50 μM DPI or (B) CSE versus CSE with 10 μM Fulvene-5 or 5. The *y*-axis = lung fluid clearance ($I-I_0$) where I represents fluid volume present at a respective point in time and I_0 is fluid volume at the first X-ray exposure. More positive values represent greater fluid clearance. n = 15 per group. Pan-Nox inhibition attenuated the effects of CSE beginning approximately 30 min after instillation ($p < 0.05$). Nox2-Nox4 inhibition significantly attenuated CSE-induced lung fluid clearance beginning at 65 min, an effect that persisted throughout the study ($p < 0.01$).

4. Discussion

Cigarette smoke and cigarette smoking are the primary etiology of chronic obstructive pulmonary disease (COPD), although the underlying molecular mechanisms that lead to disease are not completely understood. Cigarette smoke is a complex mixture of over 4700 constituents including reactive oxygen species (ROS) [22-25]. ROS serve a variety of functions and elevated levels of ROS occur in the lungs of individuals with COPD. We have shown that cigarette smoke extract (CSE) induced ROS up-regulate the epithelial sodium channel (ENaC) in alveolar epithelial cells to promote lung fluid clearance [16]. Further, CSE-induced ROS inhibited α-ENaC degradation. However, the source of ROS was unclear. The NADPH oxidases function to produce ROS and studies show that the family of Nox enzymes, in

particular Nox2 [26] and Nox4 [27], are oxygen sensors that can mediate some the reduction in ion channel activity observed under hypoxic conditions [28,29].

4.1. Single channel analysis of Nox-inhibition on CSE-induced regulation of ENaC

We have previously shown that both $O_2^{\cdot -}$ and H_2O_2 regulate ENaC activity [7,8,12,21,30-32]. Furthermore $O_2^{\cdot -}$ and H_2O_2 are present in CSE (albeit at lower concentration) and $O_2^{\cdot -}$ is produced by Nox 1-3 while H_2O_2 is thought to be produced by Nox4, DUOX1, and DUOX2. We have previously shown that by bathing alveolar epithelial cells with 400 μM glutathione we could prevent the CSE-induced up-regulation of ENaC [16]. In the current study we used a variety of Nox inhibitors to begin elucidating the role of CSE-induced, Nox-generated ROS in the regulation of ENaC. We found that Nox-generated ROS significantly contribute to ENaC activity in the setting of cigarette smoke. Due to the significant redundancy in Nox isoforms in the lung, Nox knockout models may not reliably mimic complete depletion of the functional Nox protein. For example, knockout of the $gp91^{phox}$ catalytic unit may be compensated by an increase in ROS generation by other Nox isoforms. For this reason, we opted to use currently available inhibitors that have been extensively tested and reported in the literature.

Peters and Colleagues demonstrated that Nox4, through oxidant production, plays a critical role in TGF-β trafficking of β-ENaC [33], while we have previously shown that H_2O_2 promotes membrane-retention of α-ENaC through Nedd-8 signaling in alveolar epithelial cells [31]. Perhaps the retention of α-ENaC coupled with increased ubiquitination of β-ENaC could shift membrane ENaC from a predominantly highly-selection cation (HSC) channel to a non-selective cation (NSC) channel made up of primarily α-ENaC subunits still able to transport Na^+, albeit at lower specificity for Na^+ over K^+. The potential adverse effect of shifting from HSC to NSC transport characteristics would be a significant reduction in uni-directional Na^+ transport and less efficiency in immediate lung water absorption.

4.2. Nox4 and lung pathology

Pan-Nox inhibition using DPI attenuated the CSE-induced up-regulation of ENaC in alveolar T2 cells (Figure 2). Further, inhibition of Nox 1-3 which require the small molecular weight GTPase protein Rac1 for full assembly of the regulatory subunits ($p40^{phox}$, $p47^{phox}$, and $p67^{phox}$) did not inhibit CSE-induced up-regulation of ENaC (data not shown). This suggests that Nox 4 is a major contributor to the acute effects of CSE on ENaC activity. This observation was further supported in our electrophysiological experiments (Figure 3). Moreover, Fulvene-5 inhibition attenuated the effects of CSE on α-ENaC degradation (Figure 5A and B) by inhibiting redox sensitive ubiquitination pathways (Figure 5C). Nox 4 transcript was also observed in alveolar epithelial T1 and T2 cells and Nox 4 has been localized to the plasma membrane of lung epithelial cells [34]. Indeed Nox 4 derived ROS can affect signaling pathways, and in mediating cell responses (such as survival and proliferation), Nox 4 has also been implicated in a variety of pathological states, including pulmonary fibrosis [35-37], pulmonary vascular changes associated with chronic lung disease [38], and metastatic disease [39]. Our studies indicate that Nox4 may play an important role in COPD by altering lung ENaC regulation.

4.3. Oxidative stress, inappropriate ion transport and COPD

Chronic obstructive pulmonary disease (COPD) includes chronic bronchitis and emphysema,

which afflicts the airways and alveolar airspaces, respectively. The pathogenesis of COPD is complex and incompletely understood. While it is clear that oxidative stress occurs in COPD [40], the effect of oxidative stress on ENaC activity (and whether this is the underlying cause of COPD) is an area of active research and remains unclear. Previous studies have shown that CSE alters lung epithelial lining fluid (ELF) volume by inhibiting chloride secretion and promoting dehydration of the ELF to produce a chronic bronchitis phenotype in the airways [41,42]. We propose that hyperactive Na^+ reabsorption in the distal alveolar epithelium can likewise contribute to COPD by dehydrating the ELF following cigarette smoke exposure in the airspace. Recently published reports that show spontaneous development of emphysema and chronic bronchitis in mice overexpressing β-ENaC [5] provides additional support for the role of lung ENaC in the progression of alveolar and airway disease. Moreover, airway potential difference measurements from smoker airways have increased amiloride-sensitive potential difference compared to non-smokers [43]; thus also indicating that CSE activation of ENaC in the lungs can lead to the progression of COPD.

The anti-oxidant rich epithelial lining fluid in the lungs can also impact CSE signaling to ENaC in the alveolar epithelium. We have previously shown that ENaC activity did not increase when CSE was added in the presence of a high concentration of GSH [16]. Pan-Nox inhibition inhibited the CSE-induced effects on ENaC activity. This suggests that ROS contained in the CSE serve as the initial impetus activating Noxes. We have also shown that acute exposure to CSE increases Nox 4 mRNA and transcript, which suggests that Nox 4 may play a critical role in the pathogenesis of COPD. However, additional work is needed to elucidate its role. Since Nox 4 inhibition attenuated ENaC activity and promoted proteolytic degradation of ENaC, our findings indicate that Nox 4 inhibition could be further evaluated as a therapeutic target for smoking related lung disease.

5. Conclusion

The role of ENaC in the pathogenesis of smoking-related lung disease is unclear although animal models suggest ENaC may play an important role. In the current study, we observed that the Nox 4 isoform increases lung ENaC following cigarette smoke extract exposure by increasing channel activity and half-life in the cell membrane. As such, Nox4 may be a potential therapeutic target in the treatment or prevention of smoking-related lung diseases.

Acknowledgements

We acknowledge the technical work of David Trac and Lisa Kreiner. This work was supported in part by a Parker B. Francis Fellowship and by University Research Committee/Atlanta Clinical and Translational Science Institute grant that is supported by the National Center for Advancing Translation Sciences of the National Institute of Health under award number ULTR000454 (CAD). The content is solely the responsibility of the authors and does not necessarily represent the official views of the National Institute of Health.

Conflict of interest

The authors have not conflict of interest to declare.

References

1. Eaton DC, Helms MN, Koval M, et al. (2009) The contribution of epithelial sodium channels to alveolar function in health and disease. *Annu Rev Physiol* 71: 403-423.
2. Hummler E, Barker P, Gatzy J, et al. (1996) Early death due to defective neonatal lung liquid clearance in alpha-ENaC-deficient mice. *Nat Genet* 12: 325-328.
3. Hummler E, Barker P, Talbot C, et al. (1997) A mouse model for the renal salt-wasting syndrome pseudohypoaldosteronism. *Proc Natl Acad Sci U S A* 94: 11710-11715.
4. Mall M, Grubb BR, Harkema JR, et al. (2004) Increased airway epithelial Na+ absorption produces cystic fibrosis-like lung disease in mice. *Nat Med* 10: 487-493.
5. Mall MA, Harkema JR, Trojanek JB, et al. (2008) Development of chronic bronchitis and emphysema in beta-epithelial Na+ channel-overexpressing mice. *Am J Respir Crit Care Med* 177: 730-742.
6. Mall MA (2009) Role of the amiloride-sensitive epithelial Na+ channel in the pathogenesis and as a therapeutic target for cystic fibrosis lung disease. *Exp Physiol* 94: 171-174.
7. Downs CA, Kreiner LH, Johnson NM, et al. (2015) Receptor for advanced glycation end-products regulates lung fluid balance via protein kinase C-gp91(phox) signaling to epithelial sodium channels. *Am J Respir Cell Mol Biol* 52: 75-87.
8. Goodson P, Kumar A, Jain L, et al. (2012) Nadph oxidase regulates alveolar epithelial sodium channel activity and lung fluid balance in vivo via O^{-}_{2} signaling. *Am J Physiol Lung Cell Mol Physiol* 302: L410-419.
9. Aguirre J, Lambeth JD (2010) Nox enzymes from fungus to fly to fish and what they tell us about Nox function in mammals. *Free Radic Biol Med* 49: 1342-1353.
10. Babior BM (2004) NADPH oxidase. *Curr Opin Immunol* 16: 42-47.
11. Geiszt M (2006) NADPH oxidases: new kids on the block. *Cardiovasc Res* 71: 289-299.
12. Takemura Y, Goodson P, Bao HF, et al. (2010) Rac1-mediated NADPH oxidase release of O2- regulates epithelial sodium channel activity in the alveolar epithelium. *Am J Physiol Lung Cell Mol Physiol* 298: L509-520.
13. Trac D, Liu B, Pao AC, et al. (2013) Fulvene-5 inhibition of Nadph oxidases attenuates activation of epithelial sodium channels in A6 distal nephron cells. *Am J Physiol Renal Physiol* 305: F995-F1005.
14. Barnes PJ (2014) Cellular and molecular mechanisms of chronic obstructive pulmonary disease. *Clin Chest Med* 35: 71-86.
15. Rahman I (2005) Oxidative stress in pathogenesis of chronic obstructive pulmonary disease: cellular and molecular mechanisms. *Cell Biochem Biophys* 43: 167-188.
16. Downs CA, Kreiner LH, Trac DQ, et al. (2013) Acute effects of cigarette smoke extract on alveolar epithelial sodium channel activity and lung fluid clearance. *Am J Respir Cell Mol Biol* 49: 251-259.
17. Helms MN, Self J, Bao HF, et al. (2006) Dopamine activates amiloride-sensitive sodium channels in alveolar type I cells in lung slice preparations. *Am J Physiol Lung Cell Mol Physiol* 291: L610-618.
18. Downs CA, Montgomery DW, Merkle CJ (2011) Age-related differences in cigarette smoke extract-induced H2O2 production by lung endothelial cells. *Microvasc Res* 82: 311-317.

19. Downs CA, Kreiner L, Zhao XM, et al. (2015) Oxidized glutathione (GSSG) inhibits epithelial sodium channel activity in primary alveolar epithelial cells. *Am J Physiol Lung Cell Mol Physiol* 308: L943-952.
20. Yu L, Helms MN, Yue Q, et al. (2008) Single-channel analysis of functional epithelial sodium channel (ENaC) stability at the apical membrane of A6 distal kidney cells. *Am J Physiol Renal Physiol* 295: F1519-1527.
21. Helms MN, Jain L, Self JL, et al. (2008) Redox regulation of epithelial sodium channels examined in alveolar type 1 and 2 cells patch-clamped in lung slice tissue. *J Biol Chem* 283: 22875-22883.
22. Church DF, Pryor WA (1985) Free-radical chemistry of cigarette smoke and its toxicological implications. *Environ Health Perspect* 64: 111-126.
23. Pryor WA, Prier DG, Church DF (1983) Electron-spin resonance study of mainstream and sidestream cigarette smoke: nature of the free radicals in gas-phase smoke and in cigarette tar. *Environ Health Perspect* 47: 345-355.
24. Pryor WA, Hales BJ, Premovic PI, et al. (1983) The radicals in cigarette tar: their nature and suggested physiological implications. *Science* 220: 425-427.
25. Pryor WA, Church DF, Evans MD, et al. (1990) A comparison of the free radical chemistry of tobacco-burning cigarettes and cigarettes that only heat tobacco. *Free Radic Biol Med* 8: 275-279.
26. Buttigieg J, Pan J, Yeger H, et al. (2012) NOX2 (gp91phox) is a predominant O2 sensor in a human airway chemoreceptor cell line: biochemical, molecular, and electrophysiological evidence. *Am J Physiol Lung Cell Mol Physiol* 303: L598-607.
27. Nisimoto Y, Diebold BA, Cosentino-Gomes D, et al. (2014) Nox4: a hydrogen peroxide-generating oxygen sensor. *Biochemistry* 53: 5111-5120.
28. Chen M, Xiao D, Hu XQ, et al. (2015) Hypoxia Represses ER-alpha Expression and Inhibits Estrogen-Induced Regulation of Ca2+-Activated K+ Channel Activity and Myogenic Tone in Ovine Uterine Arteries: Causal Role of DNA Methylation. *Hypertension* 66: 44-51.
29. Lai N, Lu W, Wang J (2015) Ca(2+) and ion channels in hypoxia-mediated pulmonary hypertension. *Int J Clin Exp Pathol* 8: 1081-1092.
30. Downs CA, Trac DQ, Kreiner LH, et al. (2013) Ethanol alters alveolar fluid balance via Nadph oxidase (NOX) signaling to epithelial sodium channels (ENaC) in the lung. *PLoS One* 8: e54750.
31. Downs CA, Kumar A, Kreiner LH, et al. (2013) H2O2 regulates lung epithelial sodium channel (ENaC) via ubiquitin-like protein Nedd8. *J Biol Chem* 288: 8136-8145.
32. Downs CA, Helms MN (2013) Regulation of ion transport by oxidants. *Am J Physiol Lung Cell Mol Physiol* 305: L595-603.
33. Peters DM, Vadász I, Wujak L, et al. (2014) TGF-β directs trafficking of the epithelial sodium channel ENaC which has implications for ion and fluid transport in acute lung injury. *Proc Natl Acad Sci U S A* 111: E374-383.
34. von Löhneysen K, Noack D, Jesaitis AJ, et al. (2008) Mutational analysis reveals distinct features of the Nox4-p22 phox complex. *J Biol Chem* 283: 35273-35282.
35. Amara N, Goven D, Prost F, et al. (2010) NOX4/NADPH oxidase expression is increased in pulmonary fibroblasts from patients with idiopathic pulmonary fibrosis and mediates TGFbeta1-induced fibroblast differentiation into myofibroblasts. *Thorax* 65: 733-738.

36. Boudreau HE, Casterline BW, Burke DJ, et al. (2014) Wild-type and mutant p53 differentially regulate NADPH oxidase 4 in TGF-beta-mediated migration of human lung and breast epithelial cells. *Br J Cancer* 110: 2569-2582.
37. Crestani B, Besnard V, Boczkowski J (2011) Signalling pathways from NADPH oxidase-4 to idiopathic pulmonary fibrosis. *Int J Biochem Cell Biol* 43: 1086-1089.
38. Pache JC, Carnesecchi S, Deffert C, et al. (2011) NOX-4 is expressed in thickened pulmonary arteries in idiopathic pulmonary fibrosis. *Nat Med* 17: 31-32.
39. Yan S, Liu G, Pei C, et al. (2015) Inhibition of NADPH oxidase protects against metastasis of human lung cancer by decreasing microRNA-21. *Anticancer Drugs* 26: 388-398.
40. Zinellu A, Fois AG, Sotgia S, et al. (2016) Plasma protein thiols: an early marker of oxidative stress in asthma and chronic obstructive pulmonary disease. *Eur J Clin Invest* 46: 181-188.
41. Cantin AM, Hanrahan JW, Bilodeau G, et al. (2006) Cystic fibrosis transmembrane conductance regulator function is suppressed in cigarette smokers. *Am J Respir Crit Care Med* 173: 1139-1144.
42. Kreindler JL, Jackson AD, Kemp PA, et al. (2005) Inhibition of chloride secretion in human bronchial epithelial cells by cigarette smoke extract. *Am J Physiol Lung Cell Mol Physiol* 288: L894-902.
43. Sloane P A, Shastry S, Wilhelm A, et al. (2012) A Pharmacological Approach to Acquired Cystic Fibrosis Transmembrane Conductance Regulator Dysfunction in Smoking Related Lung Disease. *PloS one* 7.

AIMS Press